Quantum Electronics **47** (11) 986–991 (2017) ©2017 Kvantovaya Elektronika and Turpion Ltd

https://doi.org/10.1070/QEL16245

Optimisation of the parameters of a broadband multibeam-pumped optical parametric amplifier

S.A. Frolov, V.I. Trunov, E.V. Pestryakov

Abstract. **We report the results of the numerical simulation of the output amplifier stage of a high-power laser system based on parametric amplification of femtosecond pulses in an LBO crystal under multibeam pumping. A technique is described for choosing an optimal amplifier configuration with an arbitrary number of pump beams to provide a wide spectral gain band with a minimum loss due to parametric diffraction. The results of simulating the parametric amplification, amplification efficiency, and spatial profile of amplified radiation with allowance for the interference of amplified parasitic beams are presented. A possibility of eliminating the spatial modulation of the amplified radiation intensity, which occurs when using spatial filters, is demonstrated. An increase in the number of pump beams is found to rise the amplified pulse duration, slightly (from 20 to 21 fs) for incoherent pump beams and more significantly (to 25 fs) for coherent beams. The amplification efficiency is reduced from 23% to 21% in the former case and to 11% in the latter case.**

Keywords: *parametric amplification, multibeam pumping, femtosecond pulses, LBO.*

1. Introduction

Laser systems based on parametric amplification stages are ones of the most promising systems for designing femtosecond radiation sources with ultrahigh intensity and contrast [1–3]. The use of parametric amplification stages with multibeam pumping makes it possible to lower the requirements to the pump pulse energy and, therefore, to increase the pulse repetition rate in ultrahigh-peak-power laser systems.

According to our preliminary analysis [4], the decisive factor in implementing broadband parametric amplification with multibeam pumping (aimed at increasing its total energy) is the choice of the pump beam incidence angles into the crystal with respect to the amplified radiation direction. In this case, the gain spectra formed by each beam should to similar in the gain region and, more specifically, should be similar to the wave mismatch curves. In the opposite case, the amplification will be much less efficient in the spectral regions with different wave mismatches due to the competition of idler waves with different phases, which will finally result in the narrowing of the total gain profile. Thus, there may be two efficient multibeam pumping regimes: with similar gain spectra and with minimally intersected spectra. This circumstance was described in a number of publications devoted to the use of two multibeam pumping regimes for parametric amplification. The first regime serves to increase the total pump energy [4–10], while the second one allows the spectral gain profile to be expanded [11–14]. Note that only narrow-band amplification was considered in the studies devoted to the first regime. It is also noteworthy that the second regime does not make it possible to increase significantly the total energy of the pump because of the small width of the spectral gain profile for additional pump beams.

To date, the maximum number of the used pump beams was five in the energy gain regime with amplification of nanosecond pulses [6] and two in the wideband gain regime with amplification of 5-fs pulses under picosecond pumping [13, 14]. Since the main purpose of this study was to develop methods for increasing the energy of 20-fs pulses at the output of a broadband parametric amplifier stage under multibeam pumping, we restrict ourselves to the consideration of only this regime.

One of the main mechanisms limiting the efficiency of multibeam pumping is parametric diffraction, or the formation and amplification of parasitic beams at the frequencies of the interacting waves: signal (amplified), idler, and pump waves. As was shown in [15], an increase in the angle between the pump beams leads to a decrease in the parametric diffraction efficiency due to the rise of the wave mismatch between the parasitic waves. The formation of parasitic waves at new sum and difference frequencies (which are primarily the second harmonics of fundamental waves) was also analysed in [7]. It was found that the degree of coherence of pump beams does not affect the efficiency of parametric amplification of the fundamental wave but suppresses the amplification of parasitic waves [9, 10]. Thus, the proper choice of a multibeam-pumped system configuration is decisive for minimising the processes of parasitic amplification with conservation of a wide spectral gain band and a high conversion factor. It is also important to perform a comparative analysis of the efficiencies of the amplification scheme with multibeam pumping and the multistage scheme of parametric amplification.

2. Optimisation of the multibeam-pumped optical parametric amplifier configuration

We elaborated a technique for determining the optimal spatial position of beams for a multibeam-pumped parametric

---

S.A. Frolov, V.I. Trunov, E.V. Pestryakov Institute of Laser Physics, Siberian Branch, Russian Academy of Sciences, prosp. Akad. Lavrent'eva 13/3, 630090 Novosibirsk, Russia;
e-mail: stanislav.a.frolov@gmail.com, trunov@laser.nsc.ru, pefvic@laser.nsc.ru

Received 28 October 2016; revision received 15 August 2017
Kvantovaya Elektronika **47** (11) 986–991 (2017)
Translated by Yu.P. Sin'kov

amplifier stage. Using this technique, we optimised the parameters of a multibeam-pumped parametric amplifier stage based on an LBO crystal for a multiterawatt two-channel laser system with coherent addition of fields, developed at the Institute of Laser Physics, Siberian Branch, Russian Academy of Sciences (SB RAS).

The technique for implementing high-efficiency parametric amplification of femtosecond pulses under multibeam pumping implies determination (in the first stage) of the optimal beam propagation directions (with respect to the amplified pulse propagation direction). A set of wavelengths is selected from the spectrum of amplified 20-fs pulse with a centre wavelength of 830 nm to search for the optimal propagation angles of the pump beam with a centre wavelength of 532 nm. These are the wavelengths 775 and 950 nm on the edges of the amplified pulse spectrum (the corresponding intensities are ~10% of the peak intensity) and 800 and 900 nm in the middle part of the pulse spectrum, with intensities exceeding 80% of the maximum value. An angular range L_n with a small wave mismatch amplitude can be put into correspondence with each wavelength λ_n. Then, obviously, the pump beams necessary for broadband amplification should lie in the range

$$M = \bigcup_n L_n,$$

i.e., in the interval of simultaneous intersection of all L_n. Then the phase-matching angle is chosen by maximising the area M. This approach makes it possible to minimise the amplification efficiency of parasitic beams because of the larger angular distance between possible directions of pump beams [15].

Our analysis showed that, at the aforementioned parameters of interacting waves in an LBO crystal in the XY plane ($\theta = 90°$), there are two optimal phase-matching angles φ (12.8° and 15.25°) for type-I phase matching. Below, we consider the XY plane and the $\boldsymbol{k}Z$ plane (where $\boldsymbol{k}$ is the wave vector of the amplified wave, lying in the XY plane) as sensitive and insensitive planes, respectively. In what follows, all beam propagation angles are counted with respect to the $\boldsymbol{k}$ vector. The ranges of angles with a small wave mismatch for each spectral component are shown grey in Fig. 1. Their intersection areas are brighter. The simultaneous intersection of the angular ranges for all spectral components is shown by white. It follows from Fig. 1 that the intersection area with a small wave mismatch for all spectral components is a ring segment in both cases. For a smaller phase-matching angle, the radius of the ring is smaller and the ring is thicker.

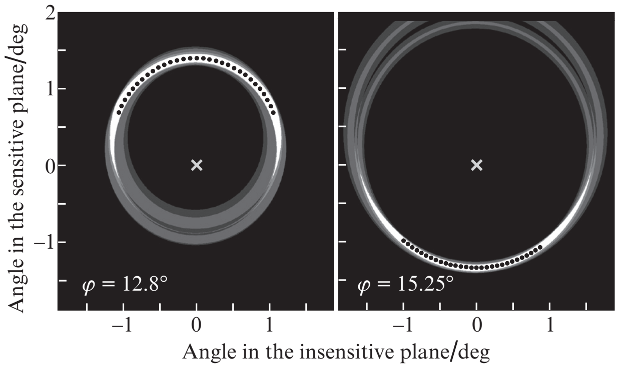

Figure 1. Wave mismatch regions with an amplitude no larger than 10 cm^{-1}: the crosses at points (0, 0) indicate the amplified beam position, and the black points show the chosen discrete sets of possible pump beam positions.

The optimal configuration of multibeam pumping is determined from the conditions for implementing the maximum wave mismatch for the amplification of parasitic components. An especially important factor is the influence of amplified parasitic beams, which arise due to the interaction between the pump beam and idler wave (the latter is formed by another pump beam and the fundamental amplified wave). With a correctly chosen pump-beam arrangement, the total pulse energy in these parasitic beams is an order of magnitude lower than in the fundamental beam because of the large wave mismatch. The parasitic beams propagate along the directions differing from the fundamental wave propagation direction and may take off a large part of the pump energy because the number of these beams is rather large. Below, the wave mismatch of the parasitic wave amplification for some set of pump beams is considered to be its minimum value among all variants of the formation of parasitic amplified waves.

Optimal pump configurations were chosen by varying possible pump-beam positions. The aforementioned ring segment was parameterised by choosing three points in the radial direction with a minimum wave mismatch amplitude of spectral components. An equidistant discrete set of pump beam positions was chosen in this segment so that they are characterised by approximately the same wave mismatch curve, allowing one to implement broadband amplification. The thus obtained set of positions is presented in Fig. 1.

Then the minimum wave mismatch of parasitic amplification processes was calculated for all possible pairs of pump beams. After that pump configurations with the largest mismatch were chosen for a specified number of pump beams. The corresponding results are listed in Table 1, and Fig. 2 shows the angular position of the pump beams. It follows from the data of Table 1 that the wave mismatch of parasitic amplification becomes sufficiently small when the number of pump beams exceeds 4–5; as will be shown below, this circumstance significantly reduces the amplification efficiency for fundamental waves. The thus found optimal position of the pump beams suggests a template for their aggregation into groups (Fig. 2). Indeed, the angles between the beams are different in the optimal configurations: there are regions of beam aggregation near the XY plane of the crystal (corresponding to a zero angle in the insensitive plane) and far from it, with the intermediate region being unfilled.

Table 1. Wave mismatch of parasitic processes for optimal multibeam-pumped configurations.

Number of beams	Wave mismatch/cm^{-1}	
	φ = 12.8°	φ = 15.25°
2	183	217
3	35.4	43.6
4	10.8	16
5	3.9	6.2
6	2.6	2.3
7	1.9	2.1

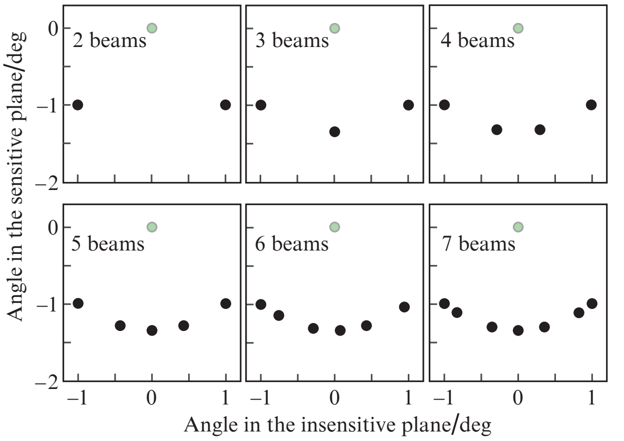

Figure 2. Versions of pump beam angular positions. Gray circles at points (0, 0) indicate the amplified beam position.

3. Model of parametric amplification with multibeam pumping

To simulate a broadband multibeam-pumped optical parametric amplifier with allowance for the parasitic generation effects, one needs a model valid both for large pump propagation angles and for wide gain bands. The best base for this simulation is the unidirectional propagation equation [16] written in the Fourier space. The only approximation for this equation is the suggestion that a pulse propagates in one direction in an isotropic medium; i.e., the energy of the backward pulse is much lower than the amplified pulse energy. The suggestion about isotropy of the medium is also used to derive the conventional truncated equations for parametric amplification [17]. To obtain a model for practical application in Eqn (26) from [16], we presented the field in the form of a sum of field envelopes (as was done in [17]) in the conventional space; we also took into account the angular dependence of the refractive index of the crystal. As a result, the system of equations has the form

$$\frac{\partial E_{\rm s}}{\partial z} = {\rm i}k_{{\rm s}z}E_{\rm s} + {\rm i}F_{+}[\sigma_{\rm s}E_{\rm i}^{*}E_{\rm p}],$$

$$\frac{\partial E_{\rm i}}{\partial z} = {\rm i}k_{{\rm i}z}E_{\rm i} + {\rm i}F_{+}[\sigma_{\rm i}E_{\rm s}^{*}E_{\rm p}], \qquad (1)$$

$$\frac{\partial E_{\rm p}}{\partial z} = {\rm i}k_{{\rm p}z}E_{\rm p} + {\rm i}F_{+}[\sigma_{\rm p}E_{\rm i}E_{\rm s}],$$

where $k_{mz} = \sqrt{\boldsymbol{k}_m^2(\omega,k_x,k_y) - k_x^2 - k_y^2}$ [the subscript $m = {\rm s, i, p}$ denotes, respectively, the amplified (signal), idler, and pump waves]; $\boldsymbol{k}_m(\omega,k_x,k_y)$ is the wave vector of wave m; the wave vector $\boldsymbol{k}_{\rm s}$ is directed along the z axis; $E_m = E_m(\omega,k_x,k_y,z)$ is the electric field strength for wave m in the Fourier space; $F_{+}[\ldots]$ is the direct time- and space-domain Fourier transform; ω is frequency; and σ_m is the nonlinear coupling coefficient. Since Eqn (1) is solved in the Fourier space, one can exactly take into account the linear effects occurring in the medium: dispersion, diffraction, and birefringence.

A specific feature of the application of system of equations (1) in simulation of multibeam pumping is that this system is solved in the angular range containing all interacting beams. In contrast to our previous calculations [4], this approach makes it possible to take into account all possible generated parasitic beams at the frequencies of all three (signal, idler, and pump) waves.

4. Multibeam pumping of optical parametric amplifiers

The sets of angular positions of pump beams, calculated using our original technique, made it possible to simulate the characteristics of the output stage of the multibeam-pumped optical parametric amplifier for the multiterawatt two-channel laser system with coherent field addition, developed at the Institute of Laser Physics SB RAS [18], using currently available pump sources. As previously [4], we consider two versions of implementing the maximum allowable total peak intensity of pump beams: (i) summation of intensities and (ii) summation of fields. The former version may occur, e. g., at different centre pump wavelengths; for this reason, it will be considered below as the case with incoherent pump beams, whereas the latter version will be treated as the case with coherent beams. In the case under consideration, with N pump beams, the energy of each 90-ps pulse was 600 mJ, and the pump beam spatial profile was approximated by a fourth-order hyper-Gaussian, with radii of $0.6N$ and $0.6N^{0.5}$ cm for peak intensity calculations with summation of fields and intensities, respectively. The peak pulse intensities in each pump beam were taken to be $8/N^2$ and $8/N$ GW cm^{-2}, respectively. To compare the efficiencies of the multibeam-pumped optical parametric amplifier and a conventional classical N-stage amplification system, we calculated the parameters of amplified pulses in the N-stage system. Two versions were considered: with intermediate telescopes for the amplified beam and without telescopes. In the scheme with telescopes in the first stage, one pump beam was used, with parameters similar to those for the multibeam scheme with $N = 1$. In further calculations, the beam size in each next stage was increased so as to make the total peak intensity of the pump and amplified beams constant at the input of each crystal. On the whole, this procedure leads to an increase in the pump beam radius to 1.3 cm in the last stage, and the length of crystals changes from 3 to 2.2 mm (7 stages) to implement the maximum gain. To obtain the maximally wide gain spectrum, an appropriate noncollinearity angle was chosen for each stage. The scheme without telescopes is on the whole similar to that with telescopes; however, the beam sizes in the first stage were chosen such as to exclude excess above the threshold total intensity (14.6 GW cm^{-2}) in the last stage. Here, the crystal lengths lied in the range from 2.5 to 5 mm.

The initial energy of the amplified pulse was 150 mJ, the duration of the chirped pulse was 40 ps, and its spectrum corresponded to a duration of 20 fs. The spatial profile of the signal beam was the same as the pump beam profile. The length of the LBO crystal was chosen so as to obtain a maximum gain.

The dependences of the calculated energies and transform-limited durations of the amplified pulse on the number of pump beams are presented in Fig. 3, along with the corresponding results for the multistage amplification system. The angular positions of the pump beams, obtained by the new method of searching for optimal schemes of a multibeam-pumped broadband parametric amplifier, provide a higher amplification efficiency with an increase in their number in comparison with the previously considered configurations [4].

For the multibeam-pumped configurations proposed in this study, an increase in the number of pump beams from one to seven only slightly (from 20 to 21 fs) increased the amplified pulse duration in the case of incoherent beams, whereas for coherent beams this value increased to 25 fs. The amplification efficiency (the ratio of the increment in the amplified pulse energy to the pump energy) decreased from 23 % to 21 % in the former case and dropped to 11 % in the latter case. The optimal crystal lengths were 3 – 10 mm for incoherent pump beams and 3 – 18 mm for coherent beams, with the number of beams ranging from one to seven.

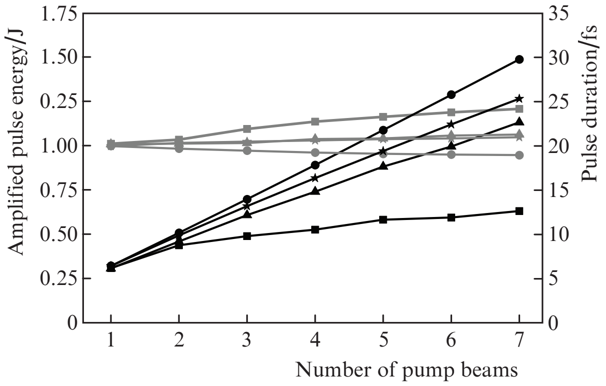

Figure 3. Energies (black curves) and transform-limited durations (gray curves) of amplified pulses with different numbers of coherent (squares) and incoherent (triangles) pump beams. The simulation results for a system of successive crystals with telescopes between stages (circles) and without telescopes (asterisks) are shown for comparison.

According to the calculation results presented in Fig. 3, the efficiency of the multistage amplification scheme, both in the versions with telescopes between stages and in the versions without telescopes, is somewhat higher, both in energy and amplified pulse duration. The reason is that the gain spectrum in the multistage scheme is wider because of the absence of the previously mentioned limitations on the choice of beam angular positions for multibeam pumping. In the case of parametric amplification of femtosecond pulses with a larger initial duration, the difference between the efficiencies of the above-considered schemes is smaller.

Figure 4 shows the angular spectra of amplified radiation for different numbers of pump beams. One can see the presence of parasitic beams, both primary (from two initially nonzero fields of the signal and pump waves) and higher order ones (from at least one initially zero field of the idler wave or other parasitic beams). The numbers of parasitic beams are significantly different for the cases with three and four pump beams. Specifically this difference is responsible for a sharp increase in the energy of parasitic beams to a rather large (more than 0.5 %–3 %) fraction of the amplified radiation energy, starting with four beams. As a result, this fraction does not exceed 3 %–4 % in the case of seven-beam pumping for coherent beams and 6 %–7 % for incoherent beams (Fig. 5). This dependence is explained by both a sharp decrease in the wave mismatch for parasitic amplification from 43.6 to 16 cm^{-1} and a rise (approximately proportionally to N^2) in the number of possible primary parasitic beams with an increase in the number of pump beams N.

Another important issue is the analysis of the formation of the amplified-beam spatial structure with allowance for the

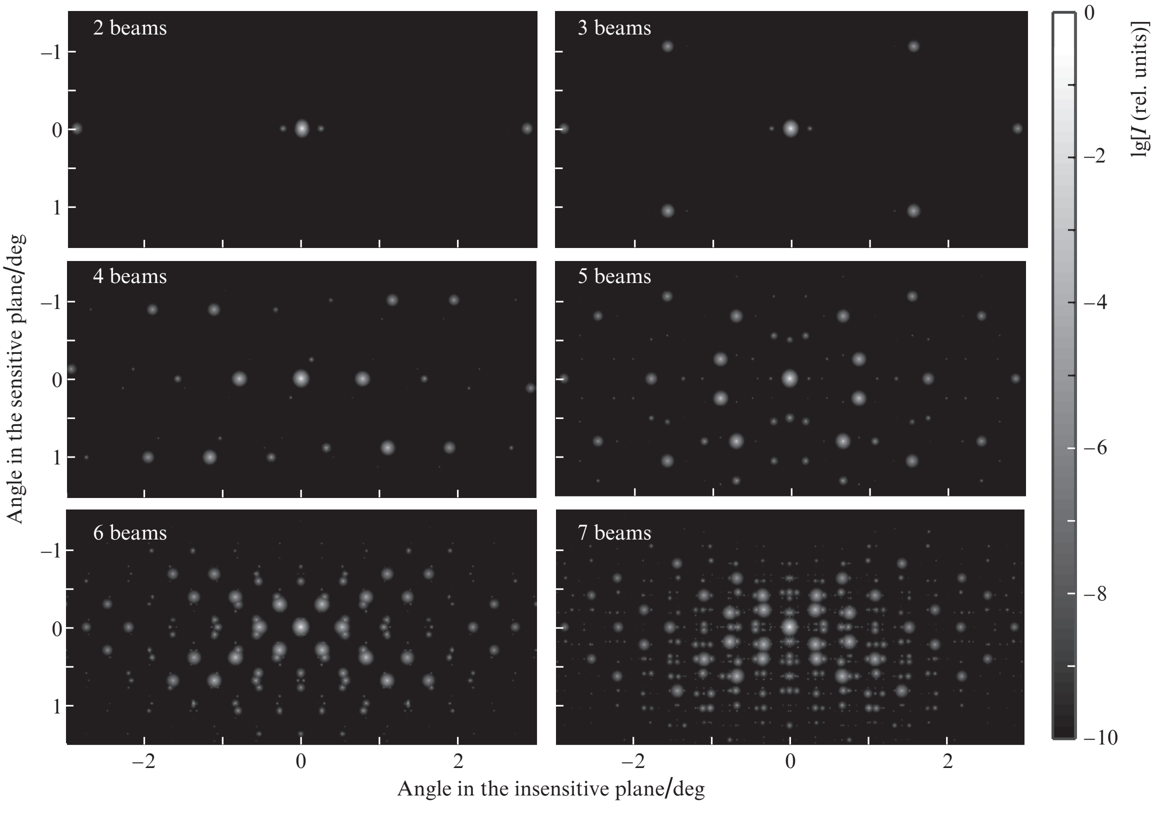

Figure 4. Angular spectra of amplified radiation with different numbers of incoherent pump beams.

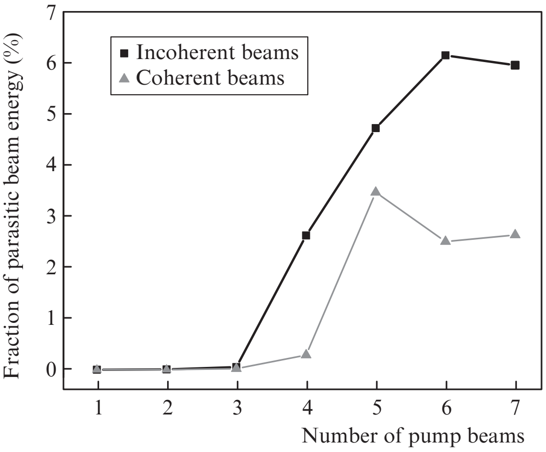

Figure 5. Dependences of the fraction of the amplified parasitic beam energy on the number of pump beams.

interference of pump beams. As was established previously, the simulated spatial profile of amplified radiation is smooth if the generation of parasitic beams is disregarded [4].

The results of our calculation with allowance for the amplification of parasitic beams show that the amplified radiation intensity is modulated in space (see Fig. 6a). A significant increase in the fraction of the parasitic beam energy with an increase in the number of pump beams to four or more leads to a significant increase in the modulation depth of the intensity distribution in the beam cross section: from few percent in the case of two or three beams to 40%–70% for four beams or more. The reason is that, despite the low intensity of parasitic beams, their number is sufficiently large to make locally their total intensity comparable with the fundamental beam intensity. This modulation can be suppressed using spatial filtering, which allows one to limit the propagation angle for the amplified radiation. A decrease in this angle, starting with 100 mrad (a value corresponding to the entire computational domain), leads to a decrease in the frequency and modulation depth with an increase in the number of filtered parasitic beams, up to its disappearance at an angle of 4 mrad, which corresponds to the region containing only the fundamental amplified beam. Figure 6b shows the amplified beam profile after spatial filtering, which provided a propagation angle of 4 mrad, excluding the presence of parasitic beams in the output radiation and, as can be seen in the figure, leading to complete suppression of modulation.

5. Conclusions

We developed a method of searching for optimal schemes of multibeam pumping of broadband parametric amplification stages based on nonlinear optical crystals, with allowance for the influence of parasitic beam generation. It is shown that, in the case of amplification of femtosecond radiation with a centre wavelength of 830 nm under 532-nm multibeam pumping, there are two optimal angles (counted from the amplified beam axis) for type-I phase matching in the XY plane of LBO crystal: 12.8° and 15.25°. Both directions, maintaining broadband amplification, differ in the efficiency of parasitic amplification processes. An original method was used to propose a series of optimal multibeam pumping schemes with a number of beams ranging from 2 to 7.

The amplification of these schemes was calculated in order to estimate the influence of parasitic amplification processes on its efficiency and the amplified pulse duration. It was found that, with an increase in the number of pump beams, the amplified pulse duration (with an initial duration of 20 fs) increases by only 5% in the case of incoherent pump beams but rises to 25 fs for coherent beams. The amplification efficiency decreases by 10% and 50% in the former and latter cases, respectively.

The numerical simulation showed that the spatial profile of the amplified radiation intensity is an interference structure, formed by the fundamental amplified beam and related parasitic beams. A possibility of suppressing the spatial modulation of the amplified radiation intensity by spatial filters was demonstrated.

The technique developed can be used to optimise (in different spectral ranges) the parametric amplification stages based on nonlinear optical crystals.

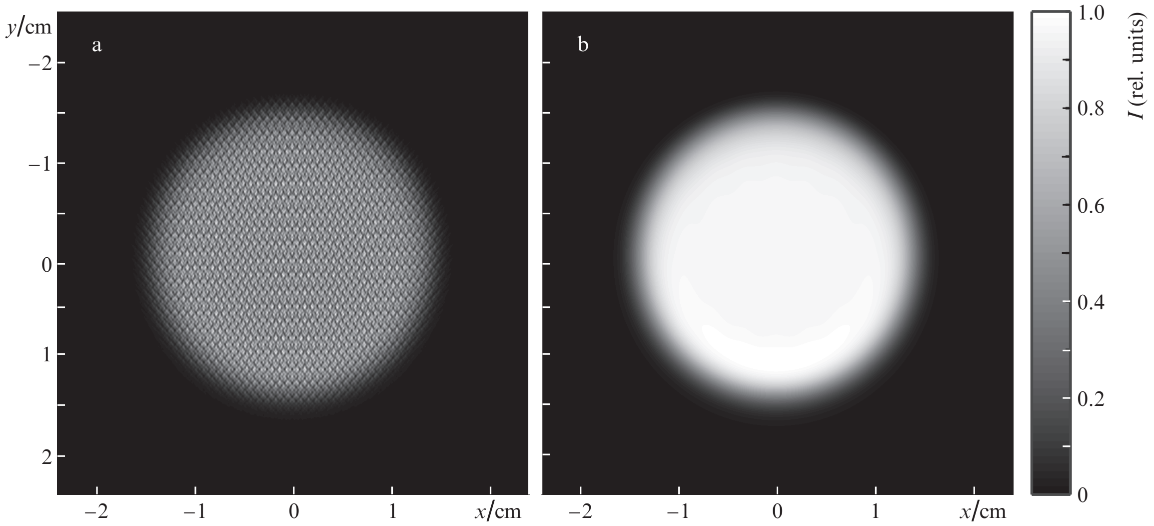

Figure 6. Spatial profile of the amplified beam under seven-beam incoherent pumping (a) before and (b) after spatial filtering.

On the whole, despite the fact that the efficiency of the multistage parametric amplification system with intermediate telescopes exceeds that of the multibeam-pumped amplification system, the latter has a number of advantages. First of all, this is the possibility of reducing the linear dimensions of the amplification system, because one stage replaces many smaller ones in this case; in addition, one nonlinear crystal is used instead of many crystals in the multistage system. Note also that each stage in the multistage system must be equipped with a telescope not only for the pump radiation but also for the amplified radiation. At the same time, the efficiency of a multistage amplification system without intermediate telescopes is comparable with that of the multibeam system, whereas the latter may be more compact.

Acknowledgements. This work was supported in part by the Presidium of the Russian Academy of Sciences ('Extreme Light Fields and Their Applications' Fundamental Research Programme) and the Russian Foundation for Basic Research (Grant No. 15-02-08917).

References

1. Lozhkarev V.V., Freidman G.I., Ginzburg V.N., Katin E.V., Khazanov E.A., Kirsanov A.V., Luchinin G.A., Mal'shakov A.N., Martyanov M.A., Palashov O.V., Poteomkin A.K., Sergeev A.M., Shaykin A.A., Yakovlev I.V. *Laser Phys. Lett.*, **4**, 421 (2007).
2. Xu L., Yu L., Liang X., Chu Y., Hu Z., Ma L., Xu Y., Wang C., Lu Xi., Lu H., Yue Y., Zhao Y., Fan F., Tu H., Leng Y., Li R., Xu Z. *Opt. Lett.*, **38**, 4837 (2013).
3. Bagayev S.N., Trunov V.I., Pestryakov E.V., Frolov S.A., Leshchenko V.E., Kokh A.E., Vasiliev V.A. *Laser Phys.*, **24**, 074016 (2014).
4. Bagayev S.N., Trunov V.I., Pestryakov E.V., Leshchenko V.E., Frolov S.A., Vasil'ev V.A. *Quantum Electron.*, **44**, 415 (2014) [*Kvantovaya Elektron.*, **44**, 415 (2014)].
5. Dubietis A., Danielius R., Tamošauskas G., Piskarskas A. *J. Opt. Soc. Am. B*, **15**, 1135 (1998).
6. Mennerat G., Trophème B., Boulanger B. *Opt. Lett.*, **38**, 3319 (2013).
7. Thlišauskas S., Butkus R., Pyragaitė V., Smilgevičius V., Stabinis A., Piskarskas A. *Opt. Commun.*, **283**, 469 (2010).
8. Pyragaite V., Butkus R., Archipovaitė G., Kezys D., Stabinis A., Piskarskas A., Smilgevičius V. *Opt.Commun.*, **309**, 344 (2013).
9. Tamošauskas G., Dubietis A., Valiulis G., Piskarskas A. *Appl. Phys. B*, **91**, 305 (2008).
10. Kurita T., Sueda K., Tsubakimoto K., Miyanaga N. *Opt. Express*, **18**, 14541 (2010).
11. Terranova F., Kiriyama H., Pegoraro F. *Opt.Commun.*, **281**, 4993 (2008).
12. Žeromskis E., Dubietis A., Tamošauskas G., Piskarskas A. *Opt. Commun.*, **203**, 435 (2002).
13. Herrmann D., Tautz R., Tavella F., Krausz F., Veisz L. *Opt. Express*, **18**, 4170 (2010).
14. Herrmann D., Homann C., Tautz R., Scharrer M., Russell P.S.J., Krausz F., Veisz L., Riedle E. *Opt. Express*, **18**, 18752 (2010).
15. Kezys D., Pyragaite V., Stabinis A., Butkus R., Smilgevičius V. *Opt. Commun.*, **324**, 58 (2014).
16. Kolesik M., Moloney J.V. *Phys. Rev. E*, **70**, 036604 (2004).
17. Bloembergen N. *Nonlinear Optics* (World Scientific, 1996).
18. Leshchenko V.E., Trunov V.I., Frolov S.A., Pestryakov E.V., Vasiliev V.A., Kvashnin N.L., Bagayev S.N. *Laser Phys. Lett.*, **11**, 095301 (2014).